FINITE ELEMENT FORMULATONS OF STRUCTURAL ACOUSTICS PROBLEMS

G. C. Everstine

Computational Mechanics (204), David Taylor Model Basin, Carderock Division,
Naval Surface Warfare Center, Bethesda, MD 20084-5000, U.S.A.

Abstract—This paper summarizes and reviews several finite element formulations used to solve structural acoustics and fluid–structure interaction problems. The fluid can be modeled using finite element formulations based on fluid pressure, displacement, velocity potential and displacement potential, each of which has advantages in different situations. In addition, finite element structural models can be coupled with either boundary element or infinite element fluid models. The formulations are applicable to a variety of applications, including acoustic cavity analyis, acoustic radiation and scattering from elastic structures vibrations of submerged structures, dynamics of fluid-filled piping systems, underwater shock analyis and transient acoustics. Published by Elsevier Science Ltd.

INTRODUCTION AND PROBLEM DEFINITION

Computational structural acoustics is concerned with the numerical prediction of the dynamic response of coupled fluid–structure systems. We restrict our interest here to fluids (e.g. water) heavy enough to influence structural response, so that a two-way coupling is required. Applications of interest include acoustic radiation from a mechanically-excited, submerged, elastic structure; acoustic scattering from a submerged, elastic structure; acoustic cavity analysis; and dynamics of fluid-filled elastic piping systems. These problems are of interest for both time-harmonic (sinusoidal) and general time-dependent (transient) excitations.

These problems have been solved by a variety of numerical techniques which differ primarily in how the fluid is modeled. Although the elastic structure (which can be very complex) is usually modeled with finite elements (including beams, plates, shells and solids), the fluid can be modeled with finite elements (with several possible formulations) [1–13], boundary elements [14–26], infinite elements [27–31], T-matrix techniques [32–34], and analytical techniques [35–37]. In addition, various combinations of these techniques have been used. Many of these approaches will be discussed in this paper, although the primary emphasis will be on the finite element modeling of fluid domains. Although there are no new formulations introduced here, this paper summarizes and characterizes, using a consistent notation, several different formulations for a variety of related applications. Most of the finite element formulations will be presented in the time domain, so that they are also applicable for frequency domain analysis. Because of the length of this paper, only formulations will be discussed. Examples can be found in the references.

The commonality among the applications listed above is the mathematical model. The structure, if it can be assumed to remain elastic, behaves according to the theory of elasticity [38] and the various approximate engineering theories for beams, plates, and shells. The fluid is treated as a compressible, inviscid, nonflowing medium whose pressure satisfies the wave equation [39, 40]

$$\nabla^2 p = \ddot{p}/c^2, \tag{1}$$

where ∇^2 is the Laplacian operator, p is the dynamic fluid pressure (the excess above ambient), c is the wave speed in the fluid, and dots denote partial differentiation with respect to time. This equation also assumes an adiabatic process, local density changes which are small, and small amplitude displacement and velocity of the fluid particles. Boundary conditions include the rigid wall condition,

$$\frac{\partial p}{\partial n} = 0 \tag{2}$$

(where n is the normal), and the pressure-release condition, $p = 0$. At a free surface where surface waves are of interest, the linearized free surface condition is

$$\frac{\partial p}{\partial n} = -\ddot{p}/g \tag{3}$$

where g is the acceleration due to gravity. Free surface waves are rarely of interest in structural

acoustics applications, since the frequencies associated with fluid-loaded elastic vibrations are generally much higher than those associated with water waves. Thus, from the point of view of free surface water waves, the pressure-release boundary condition, $p = 0$, can be referred to as a "high frequency" boundary condition, whereas Eqn (3) is a low frequency boundary condition

At an accelerating boundary (a fluid–structure interface), momentum and continuity considerations require that

$$\frac{\partial p}{\partial n} = -\rho \ddot{u}_n, \qquad (4)$$

where ρ is the fluid density, and $\ddot{u}_n$ is the normal component of fluid particle acceleration. This condition expresses the effect of structural motion on the fluid. The effect of fluid pressure on the structure is imposed as a load, proportional to pressure, applied to the wet surface of the structure.

Since fluid pressure is a scalar potential, the fluid could alternatively be formulated in terms of other potentials, including velocity potential [10, 11] (whose gradient is velocity) and displacement potential [8] (whose gradient is displacement), which also satisfy the wave equation. The fluid displacement potential, for example, has been used as the fundamental fluid unknown for transient shock-induced cavitation problems [8].

For time-harmonic excitation, for which the time dependence is $e^{i\omega t}$, the wave equation (1) becomes the Helmholtz equation

$$\nabla^2 p + k^2 p = 0. \qquad (5)$$

where ω is the circular frequency, p now represents the complex amplitude of pressure, and $k = \omega/c$ is the acoustic wavenumber. We note that the convention commonly used in structural dynamics, $e^{i\omega t}$, differs from that commonly used in acoustics and electromagnetics, $e^{-i\omega t}$.

The general fluid–structure interaction problem therefore requires the coupled solution of the elastic structure equations, the fluid equation [eqn (1) or eqn (5)], and the interface conditions [eqn (4) and the fluid pressure loading on the structure].

FLUID FINITE ELEMENTS

A standard finite element discretization of the wave equation, based on a variational principle or the method of weighted residuals (Galerkin's method), yields, in the time domain, element equations of the form [1, 41]

$$Q^{(e)}\ddot{p} + H^{(e)}p = 0, \qquad (6)$$

where the terms in the matrices $H^{(e)}$ and $Q^{(e)}$ are given by

$$h_{ij} = \int_\Omega \left[\frac{\partial N_i}{\partial x}\frac{\partial N_j}{\partial x} + \frac{\partial N_i}{\partial y}\frac{\partial N_j}{\partial y} + \frac{\partial N_i}{\partial z}\frac{\partial N_j}{\partial z} \right] d\Omega \quad (7)$$

and

$$q_{ij} = \frac{1}{c^2}\int_\Omega N_i N_j \, d\Omega, \qquad (8)$$

where Ω is the domain of an element, and N_i is the element shape function associated with grid point i.

Fluid finite elements can alternatively be created from elastic finite elements by observing the analogy [42] between the wave equation (1) and the equations of elasticity. The x-component of the Navier equations of elasticity, which are the equations solved by structural analyis computer programs, is

$$\frac{\lambda + 2G}{G} u_{,xx} + u_{,yy} + u_{,zz} + \frac{\lambda + G}{G}(v_{,xy} + w_{,xz})$$

$$+ \frac{1}{G}f_x = \frac{\rho}{G}\ddot{u}, \quad (9)$$

where u, v and w are the Cartesian components of displacement, λ is a Lamé elastic constant, G is the shear modulus, f_x is the x-component of body force per unit volume (e.g. gravity), ρ is the mass density, and commas denote partial differentiation. A comparison of eqns (1) and (9) indicates that elastic finite elements can be used to model scalar pressure fields if we let u, the x-component of displacement, represent p, set $v = w = 0$ everywhere, $f_x = 0$, and $\lambda = -G$. For three-dimensional analysis, the isotropic engineering constants consistent with this last requirement are [42]

$$E_e = 10^{20}G_e, \quad \rho_e = G_e/c^2, \qquad (10)$$

where the element shear modulus G_e can be selected arbitrarily. The subscript "e" has been added to these constants to emphasize that they are merely numbers assigned to the elements.

Under this analogy, the pressure gradient $\partial p/\partial n$ can be prescribed at a (fluid) boundary point by applying a "force" to the fluid d.f. at that point equal to $G_e A \, \partial p/\partial n$, where A is the (consistent or lumped) area assigned to the point, and n is the outward normal from the fluid domain [42]. As expected, the Neumann condition $\partial p/\partial n = 0$ is the natural boundary condition.

A finite element model of an infinite fluid domain needs to be truncated at an artificial boundary, where a nonreflecting (wave-absorbing) boundary condition must be imposed. Since the mathematically

exact absorbing boundary condition is nonlocal in both space and time (for transient problems), approximate conditions are generally used. The simplest approximate radiation boundary condition [12, 43, 44] are the plane wave condition,

$$\frac{\partial p}{\partial n} = -\frac{\dot{p}}{c},\tag{11}$$

and the next higher order condition, the curved wave absorbing boundary condition,

$$\frac{\partial p}{\partial n} = -\frac{\dot{p}}{c} - \frac{p}{r},\tag{12}$$

where r is the radius of the boundary. Both these boundary conditions are local in both space and time. Under the acoustic–elastic analogy [42], eqn (11) is implemented by attaching a "dashpot" between each fluid boundary point and ground; eqn (12) is implemented by attaching a "spring" and "dashpot" in parallel between each fluid boundary point and ground. Both these conditions have the effect of adding a "damping" matrix to the matrix equations for the fluid domain.

To summarize, the wave equation (eqn (1)) can be solved with elastic finite elements if the three-dimensional region is modeled with three-dimensional solid finite elements (e.g. isoparametric bricks or axisymmetric solids of revolution) having material properties given by eqn (10), and only one of the three Cartesian components of displacement is retained to represent the scalar variable p [42]. In Cartesian coordinates, any of the three components can be used. The solution of axisymmetric problems in cylindrical coordinates follows the same approach except that the z-component of displacement is the only one which can be used to represent p.

One motivation for using the acoustic–elastic analogy is that standard structural dynamics codes can be used to solve the coupled fluid–structure problem. From an engineering point of view, it is convenient to make use of existing general purpose codes, because of their wide availability, versatility, reliability, consultative support, and abundance of pre- and postprocessors.

RADIATION AND SCATTERING FROM ELASTIC STRUCTURES

In the scattering problem, a submerged elastic body is subjected to a plane wave incident loading, as shown in Fig. 1. For the time-harmonic case, the excitation has a single prescribed circular frequency ω. For the time-dependent (transient) case, the prescribed pressure loading is an arbitrary function of time. Without loss of generality, we can assume that the incident wave propagates in the negative z-direction. The speed of such propagation is c, the speed of sound in the fluid.

Within the fluid region, the total pressure p satisfies the wave equation, eqn (1). Since the incident free-field pressure p_i, is known, it is convenient to decompose the total pressure p into the sum of incident and scattered pressures [11].

$$p = p_i + p_s,\tag{13}$$

each of which satisfies the wave equation. (By definition, the incident free-field pressure is that pressure which would occur in the fluid in the absence of any scatterer.)

We now formulate the problem for finite element solution. Consider an arbitrary, submerged, three-dimensional elastic structure subjected to either internal time-dependent loads or an external time-dependent incident pressure. If the structure is modeled with finite elements, the resulting matrix equation of motion for the structural degrees of freedom is

$$\mathbf{M\ddot{u} + B\dot{u} + Ku = F - GAp},\tag{14}$$

where $\mathbf{M}$, $\mathbf{B}$ and $\mathbf{K}$ are the structural mass, viscous damping and stiffness matrices (dimension $s \times s$), respectively, $\mathbf{u}$ is the displacement vector for all structural d.f. (wet and dry) in terms of the coordinate systems selected by the analyst ($s \times r$), $\mathbf{F}$ is the vector of applied mechanical forces applied to the structure ($s \times r$), $\mathbf{G}$ is the rectangular transformation matrix of direction cosines to transform a vector of outward normal forces at the wet points to a vector of forces at all points in the coordinate systems selected by the analyst ($s \times f$), $\mathbf{A}$ is the (diagonal or consistent) area matrix for the wet surface ($f \times f$), $\mathbf{p}$ is the vector of total fluid pressures (incident + scattered) applied at the wet grid points ($f \times r$), and dots denote differentiation with respect to time. The pressure $\mathbf{p}$ is assumed positive in compression. In the above dimensions, s denotes the total number of independent structural d.f. (wet and dry), f denotes the number of fluid d.f. (the number of wet points), and r denotes the number of load cases. The matrix product $\mathbf{GA}$ can be interpreted as the matrix which converts a vector of negative fluid pressures to structural loads in the global coordinate

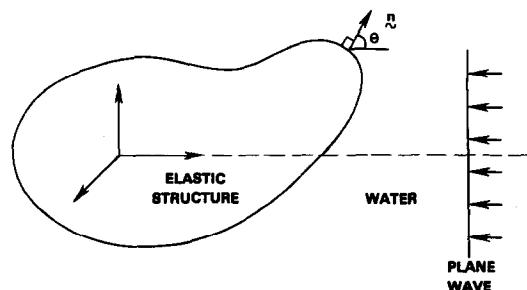Fig. 1. The scattering problem.

system. The last two equations can be combined to yield

$$\mathbf{M\ddot{u}} + \mathbf{B\dot{u}} + \mathbf{Ku} + \mathbf{GAp_s} = \mathbf{F} - \mathbf{GAp_i}. \quad (15)$$

A finite element model of the exterior fluid domain (with scattered pressure $\mathbf{p_s}$ as the fundamental unknown) results in a matrix equation of the form

$$\mathbf{Q\ddot{p}_s} + \mathbf{C\dot{p}_s} + \mathbf{Hp_s} = \mathbf{F^{(p)}}, \quad (16)$$

where $\mathbf{p_s}$ is the vector of scattered fluid pressures at the grid points of the fluid region, $\mathbf{Q}$ and $\mathbf{H}$ are the finite element system matrices for the fluid domain [as defined in eqns (6)–(8)], $\mathbf{C}$ is the "damping" matrix arising from the radiation boundary condition [e.g., eqn (11)] and $\mathbf{F^{(p)}}$ is the "loading" applied to fluid d.f. due to the fluid–structure interface condition, eqn (4). Using the acoustic–elastic analogy, structural finite elements can be used to model both structural and fluid regions. Material constants assigned to the elastic elements used to model the fluid are specified according to eqn (10). In three dimensions, elastic solid elements are used (e.g. isoparametric bricks for general three-dimensional analysis or solids of revolution for axisymmetric analysis).

At the fluid-structure interface, eqns (4) and (13) can be combined to yield

$$\frac{\partial p_s}{\partial n} = \rho(\ddot{u}_{ni} - \ddot{u}_n), \quad (17)$$

where n is the outward unit normal, and $\ddot{u}_{ni}$ and $\ddot{u}_n$ are, respectively, the incident and total outward normal components of fluid particle acceleration at the interface. Thus, from the analogy, we impose the fluid–structure interface condition by applying a "load" to each interface fluid point given by

$$\mathbf{F^{(p)}} = -\rho G_e \mathbf{A}(\ddot{u}_{ni} - \ddot{u}_n), \quad (18)$$

where the first minus sign is introduced since, in the coupled problem, we choose n as the outward normal from the structure into the fluid, making n an inward normal for the fluid region. The normal displacements $\mathbf{u_n}$ are related to the total displacements $\mathbf{u}$ by the same rectangular transformation matrix $\mathbf{G}$ used above

$$\mathbf{u_n} = \mathbf{G^T u}, \quad (19)$$

where T denotes the matrix transpose. Equations (16), (18) and (19) can be combined to yield

$$\mathbf{Q\ddot{p}_s} + \mathbf{C\dot{p}_s} + \mathbf{Hp_s} - \rho G_e (\mathbf{GA})^T \ddot{\mathbf{u}} = -\rho G_e \mathbf{A\ddot{u}_{ni}}. \quad (20)$$

If the arbitrary fluid element "shear modulus" G_e is now defined as $G_e = 1$, and eqns (15) and (20) are combined into one overall matrix system, we obtain

the so-called pressure formulation for the coupled fluid–structure problem

$$\begin{bmatrix} \mathbf{M} & \mathbf{0} \\ -\rho \mathbf{L}^T & \mathbf{Q} \end{bmatrix} \begin{Bmatrix} \ddot{\mathbf{u}} \\ \ddot{\mathbf{p}}_s \end{Bmatrix} + \begin{bmatrix} \mathbf{B} & \mathbf{0} \\ \mathbf{0} & \mathbf{C} \end{bmatrix} \begin{Bmatrix} \dot{\mathbf{u}} \\ \dot{\mathbf{p}}_s \end{Bmatrix}$$

$$+ \begin{bmatrix} \mathbf{K} & \mathbf{L} \\ \mathbf{0} & \mathbf{H} \end{bmatrix} \begin{Bmatrix} \mathbf{u} \\ \mathbf{p}_s \end{Bmatrix} = \begin{Bmatrix} \mathbf{F} - \mathbf{Lp_i} \\ -\rho \mathbf{A\ddot{u}_{ni}} \end{Bmatrix}, \quad (21)$$

where $\ddot{u}_{ni}$ is the outward normal component of incident fluid particle acceleration, and the fluid–structure coupling matrix $\mathbf{L}$ is given by

$$\mathbf{L} = \mathbf{GA}. \quad (22)$$

The right-hand side of eqn (21) has contributions from both mechanical ($\mathbf{F}$) and incident pressure ($\mathbf{p_i}$ and $\ddot{u}_{ni}$) loadings. The incident pressure excites points only on the fluid–structure interface. For scattering problems, the mechanical load $\mathbf{F}$ is zero. For radiation problems, $\mathbf{F}$ is nonzero, and the incident pressure $\mathbf{p_i}$ and the incident fluid particle acceleration both vanish. Notice that the pressure formulation (eqn (21)) is unsymmetric.

The coupled fluid–structure matrix system can be symmetrized by defining a new fluid unknown q such that

$$\mathbf{q} = \int_0^t \mathbf{p_s} \, dt, \quad \dot{\mathbf{q}} = \mathbf{p_s}, \quad (23)$$

If eqn (20) is integrated in time, and the arbitrary fluid element "shear modulus" G_e is chosen as

$$G_e = -1/\rho \quad (24)$$

(i.e. if the fluid partition is muliplied by $-1/\rho$), we obtain the symmetric velocity potential formulation of the coupled fluid–structure problem [10, 11]

$$\begin{bmatrix} \mathbf{M} & \mathbf{0} \\ \mathbf{0} & \mathbf{Q} \end{bmatrix} \begin{Bmatrix} \ddot{\mathbf{u}} \\ \ddot{q} \end{Bmatrix} + \begin{bmatrix} \mathbf{B} & \mathbf{L} \\ \mathbf{L}^T & \mathbf{C} \end{bmatrix} \begin{Bmatrix} \dot{\mathbf{u}} \\ \dot{q} \end{Bmatrix}$$

$$+ \begin{bmatrix} \mathbf{K} & \mathbf{0} \\ \mathbf{0} & \mathbf{H} \end{bmatrix} \begin{Bmatrix} \mathbf{u} \\ q \end{Bmatrix} = \begin{Bmatrix} \mathbf{F} - \mathbf{Lp_i} \\ \mathbf{Av}_{ni} \end{Bmatrix}, \quad (25)$$

where v_{ni} ($= \dot{u}_{ni}$) is the outward normal component of incident fluid particle velocity at the fluid–structure interface. The new variable q is, except for a muliplicative constant, the velocity potential ϕ, since, from Bernoulli's equation,

$$p = -\rho \frac{\partial \phi}{\partial t}. \quad (26)$$

Equation (25) could also be recast in terms of ϕ rather than q as the fundamental fluid unknown, but no particular advantage would result. In fact, the use of q rather than ϕ has the practical advantage that the fluid pressure can be recovered directly from the finite element program as the time derivative (velocity) of the unknown q.

The only effect on the coupled fluid–structure equations of switching from pressure to velocity potential as the fundamental unknown has been to move the coupling matrix $\mathbf{L}$ from the mass and stiffness parts of the problem to the damping part of the problem (although $\mathbf{L}$ introduces no damping). If a problem already has damping present from another source (e.g. structural or radiation damping), the reformulation has yielded symmetric matrices with no penalty.

For the direct integration of undamped ($\mathbf{B} = \mathbf{C} = \mathbf{0}$) time-dependent problems, the reformulation results in a net gain for two reasons. First, a nonsymmetric, real problem had been converted to a symmetric, real problem. The only price paid for the conversion is that the coefficient matrices involved in the direct integration algorithm (e.g. Newmark method) now involve linear combinations of mass, stiffness and damping rather than only mass and stiffness. The second reason for preferring the reformulation for transient problems is that, for scattering problems, the right-hand side excitation applied to the fluid partition is proportional to the incident fluid particle velocity rather than acceleration. Incident loadings with a pressure jump discontinuity (a common occurence in underwater shock problems) also have a particle velocity jump discontinuity and thus a particle acceleration discontinuity which is a Dirac delta function. Since at every fluid–structure interface point the Dirac delta function would occur at a different time, the impulsive right-hand side cannot simply be replaced by nonzero initial conditions on $\dot{p}$. Thus numerical difficulties associated with treating Dirac delta functions are eliminated by switching to the velocity potential formulation.

On the other hand, for forced time-harmonic problems which are undamped ($\mathbf{B} = \mathbf{C} = \mathbf{0}$), the reformulation results in a system more costly to solve, because the time-harmonic form of the pressure formulation, eqn (21), requires a non-symmetric, real solution algorithm, in contrast to the symmetric, complex solver required by the time-harmonic form of the symmetric velocity potential formulation, eqn (25) (with $\mathbf{B} = \mathbf{C} = \mathbf{0}$). Symmetric, complex solvers generally require about twice as much computer time as unsymmetric, real solvers.

To summarize, both structural and fluid domains are modeled with finite elements. For the fluid domain, the material constants assigned to the (elastic, isotropic) finite elements are

$$E_e = -10^{20}/\rho, \quad G_e = -1/\rho,$$

$$\rho_e = -1(\rho c^2), \tag{27}$$

where E_e, G_e and ρ_e are the Young's modulus, shear modulus and mass density, respectively, assigned to the fluid finite elements. The properties ρ and c above are the actual density and sound speed for the fluid medium. The radiation boundary condition used is, for example, the plane wave approximation, eqn (11), which is adequate if the outer fluid boundary is sufficiently far from the structure [3, 9]. With this boundary condition, matrix $\mathbf{C}$ in eqn (25) arises from dashpots applied at the outer fluid boundary with damping constant $-A/(\rho c)$ at each grid point to which the area A has been assigned. The coupling matrix $\mathbf{L}$ is the matrix which converts a vector of negative fluid pressures to structural loads in the global coordinate system.

The right-hand side of eqn (25) can often be simplified further, since, for plane waves propagating in the negative z-direction at speed c, the incident free-field pressure and incident fluid particle velocity in the z-direction are related by [45]

$$p_i = -\rho c v_{zi}. \tag{28}$$

Then, like in Fig. 1, if we define θ as the angle between the normal n and the positive z-axis,

$$v_{ni} = v_{zi} \cos \theta = -p_i \cos \theta/(\rho c). \tag{29}$$

For plane waves, the z-component of the free-field fluid particle velocity v_{zi} is the same at all points in space except for a time delay, which depends only on the z-coordinate of the points. Thus, for plane incident waves, eqn (25) can alternatively be written

$$\begin{bmatrix} \mathbf{M} & \mathbf{0} \\ \mathbf{0} & \mathbf{Q} \end{bmatrix} \begin{Bmatrix} \ddot{\mathbf{u}} \\ \ddot{\mathbf{q}} \end{Bmatrix} + \begin{bmatrix} \mathbf{B} & \mathbf{L} \\ \mathbf{L}^T & \mathbf{C} \end{bmatrix} \begin{Bmatrix} \dot{\mathbf{u}} \\ \dot{\mathbf{q}} \end{Bmatrix}$$

$$+ \begin{bmatrix} \mathbf{K} & \mathbf{0} \\ \mathbf{0} & \mathbf{H} \end{bmatrix} \begin{Bmatrix} \mathbf{u} \\ \mathbf{q} \end{Bmatrix} = \begin{Bmatrix} \mathbf{F} - \mathbf{L}p_i \\ -\mathbf{A}p_i \cos \theta/(\rho c) \end{Bmatrix}, \tag{30}$$

We note that the structural and fluid unknowns are not sequenced, as perhaps implied by the partitioned form of eqns (21), (25) and (30). The coupling matrix $\mathbf{L}$ is quite sparse and, if computed using a "lumped" formulation, has nonzeros only for matrix rows associated with the structural dof at the fluid–structure interface and columns associated with the coincident fluid points. Thus, the grid points should be sequenced for minimum matrix bandwidth or profile (as appropriate for the finite element program being used) as if the structural and fluid meshes

comprised a single large mesh. As a result, the structural and fluid grid points will, in general, be interspersed in their numbering, and the system matrices will be sparse and banded.

FLUID DISPLACEMENT FORMULATION

Although the state of the fluid at a point is definable with a single scalar potential, it is possible (and sometimes convenient) to use instead the fluid displacement, a vector with three components, as the fundamental unknown in the fluid domain [3–5, 7, 9, 13]. An isotropic elastic solid can be configured to represent a compressible, inviscid fluid if the shear modulus is set to zero, and the three direct stresses are all equal and given by

$$\sigma_{xx} = \sigma_{yy} = \sigma_{zz} = B(\epsilon_{xx} + \epsilon_{yy} + \epsilon_{zz}), \qquad (31)$$

where $B = \rho c^2$ is the bulk modulus of the fluid, and ϵ_{xx}, ϵ_{yy} and ϵ_{zz} are the Cartesian components of normal strain. Although these constitutive relations can be specified exactly, they can also be approximated using the engineering constants (Young's modulus and Poisson's ratio)

$$E_e = (6\alpha)\rho c^2, \quad v_e = \tfrac{1}{2} - \alpha, \qquad (32)$$

where α should be small, but not numerically insignificant compared to unity (e.g. $\alpha = 10^{-4}$). At each fluid–structure interface point, two grids are assigned (one for the structure and one for the fluid), with continuity enforced on the normal displacement. The tangential displacement is generally unconstrained (a slip condition).

The principal advantage of the displacement formulation compared to the scalar potential formulations is that the fluid–structure interface condition is easier to implement with standard finite element computer programs. In fact, to simplify the implementation even further, some practitioners impose a no-slip condition at the fluid–structure interface, in which a case a single grid point can be used to represent both structure and fluid displacement at each interface location.

The principal disadvantages of the displacement formulation are that the fluid domain has three times as many unknowns (with a corresponding increase in matrix bandwidth or profile), and the small or zero shear modulus induces spurious modes, a situation which can be bothersome in time-harmonic problems, either forced or unforced. Hamdi and Ousset [7] showed that the spurious modes, which are scattered throughout the frequency spectrum of interest, can be eliminated by enforcing irrotationality on the fluid displacement. Chen and Taylor [13] showed that these modes can alternatively be eleminated by using reduced integration in the stiffness calculation in combination with a projection on the element mass matrix.
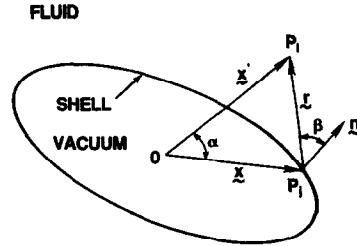

Fig. 2. Notation for Helmholtz integral equation.

Finite element practitioners sometimes claim that the spurious modes, which have short wavelengths, do not cause difficulties in time-dependent problems; the author is not aware of a study supporting this conclusion.

TIME-HARMONIC FLUID BOUNDARY ELEMENT MODELING

For time-harmonic problems, with time dependence $e^{i\omega t}$, eqn (14) becomes

$$\mathbf{Yu} = \mathbf{F} - \mathbf{GAp}, \qquad (33)$$

where

$$\mathbf{Y} = -\omega^2\mathbf{M} + i\omega\mathbf{B} + \mathbf{K}, \qquad (34)$$

and ω is the circular frequency of excitation. For structures with a nonzero loss factor, $\mathbf{K}$ is complex. In addition, $\mathbf{K}$ can include the geometric stiffness effects of hydrostatic pressure, if any [46].

The basis for a fluid boundary element model is the integral form [19] of the Helmholtz equation, eqn (5)

$$\int_S p(\mathbf{x}) \frac{\partial D(r)}{\partial n} \, dS - \int_S \hat{q}(\mathbf{x}) D(r) \, dS$$

$$= \begin{cases} p(\mathbf{x}')/2 - p_1, & \mathbf{x}' \text{ on } S, \\ p(\mathbf{x}') - p_1, & \mathbf{x}' \text{ in } E, \quad (35) \\ -p_1, & \mathbf{x}' \text{ in } I, \end{cases}$$

where S, E and I denote surface, exterior and interior fluid points, respectively, p_1 is the incident free-field pressure, r is the distance from $\mathbf{x}$ to $\mathbf{x}'$ (Fig. 2), D is the free-space Green's function

$$D(r) = \frac{e^{-ikr}}{4\pi r}, \qquad (36)$$

$$\hat{q} = \frac{\partial p}{\partial n} = \omega^2 \rho u_n, \qquad (37)$$

ρ is the mass density of the fluid, and u_n is the outward normal component of displacement on S. As shown in Fig. 2, $\mathbf{x}$ in eqn (35) is the position vector

for a typical point P_j on the surface S, $\mathbf{x}'$ is the position vector for the point P_i which may be either on the surface or in the exterior field E, the vector $\mathbf{r} = \mathbf{x}' - \mathbf{x}$, and $\mathbf{n}$ is the unit outward normal at P_j. We denote the lengths of the vectors $\mathbf{x}$, $\mathbf{x}'$, and $\mathbf{r}$ by x, x', and r, respectively. The normal derivative of the Green's function D appearing in eqn (35) is

$$\frac{\partial D(r)}{\partial n} = \frac{\mathrm{e}^{-\mathrm{i}kr}}{4\pi r}\left(ik + \frac{1}{r}\right)\cos\beta, \qquad (38)$$

where β is defined as the angle between the normal $\mathbf{n}$ and the vector $\mathbf{r}$, as shown in Fig. 2.

All three integral equations in eqn (35) are needed for exterior fluids. The surface equation provides the fluid impedance at the fluid–structure interface. Since the surface equation exhibits nonuniqueness at certain discrete characteristic frequencies [15, 17], the interior equation can be used to provide additional constraint equations which ensure the required uniqueness. The exterior equation is used to compute the exterior pressure field once the surface solution (which includes the fluid pressure and its gradient) is known. We note that the right-hand side of the exterior equation is equal to p_s, the scattered pressure.

The substitution of the last three equations into the surface equation, eqn (35a), yields

$$\frac{p(\mathbf{x}')}{2} - \int_S p(\mathbf{x})\frac{\mathrm{e}^{-\mathrm{i}kr}}{4\pi r}\left(ik + \frac{1}{r}\right)\cos\beta\,\mathrm{d}S$$

$$= -\omega^2\rho\int_S u_n(\mathbf{x})\frac{\mathrm{e}^{-\mathrm{i}kr}}{4\pi r}\,dS + p_1, \quad \mathbf{x}' \text{ on } S. \quad (39)$$

This integral equation relates the total pressure p and normal displacment u_n on S. If eqn (39) is discretized for numerical computation, we obtain the matrix equation

$$\mathbf{E}\mathbf{p} = -\omega^2\mathbf{C}\mathbf{u}_n + \mathbf{p}_1 \qquad (40)$$

on S, where vector $\mathbf{p}$ (of dimension $f \times r$) is the vector of complex amplitudes of the pressure on the structure's wet surface, matrices $\mathbf{E}$ and $\mathbf{C}$ (both $f \times f$) are fully-populated, complex, nonsymmetric, and frequency-dependent, and vector $\mathbf{p}_1(f \times r)$ is the complex amplitude of the incident pressure vector. The number of unknowns in this system is f, the number of wet points on the fluid–structure interface; r denotes the number of load cases.

If displacements $\mathbf{u}$ and $\mathbf{u}_n$ are eliminated from eqns (33), (40) and (19), the resulting equation for coupled fluid–structure system is [25]

$$(\mathbf{E} - \omega^2\mathbf{C}\mathbf{G}^\mathsf{T}\mathbf{Y}^{-1}\mathbf{G}\mathbf{A})\mathbf{p} = -\omega^2\mathbf{C}\mathbf{G}^\mathsf{T}\mathbf{Y}^{-1}\mathbf{F} + \mathbf{p}_1. \quad (41)$$

This equation can be solved for the vector $\mathbf{p}$ of surface pressures, since the rest of the equation depends only on the geometry, the material properties, and the frequency. Since the two right-hand side terms in eqn (41) correspond to mechanical and incident loadings, only one of the two terms would ordinarily be present for a given case. This matrix system is complex, full, nonsymmetric and frequency-dependent. Although asymptotically (i.e. for very large problems) the solution of eqn (41) might be the most time-consuming operation, in practice the presence of internal structure increases the order and wavefront of the structural matrix $\mathbf{Y}$, so that forming $\mathbf{Y}^{-1}\mathbf{G}\mathbf{A}$ often requires the most time [25].

The displacement vector $\mathbf{u}$ for all structural d.f. is recovered by solving eqn (33) for $\mathbf{u}$, and the surface normal displacement vector $\mathbf{u}_n$ is recovered by substituting this solution for $\mathbf{u}$ into eqn (19).

With the solution for the pressures and displacements on the surface, the pressures radiated or scattered at points $\mathbf{x}'$ in the exterior domain can be obtained by integrating the exterior form of the Helmholtz integral equation (expressed here in asymptotic far-field form [25])

$$p(\mathbf{x}') = \frac{\mathrm{i}k\mathrm{e}^{\mathrm{i}kx'}}{4\pi x'}\int_S [\rho c v_n(\mathbf{x}) + \mathbf{p}(\mathbf{x})\cos\beta]\mathrm{e}^{\mathrm{i}kx\cos\alpha}\,\mathrm{d}S,$$

$$\mathbf{x}' \text{ in } \mathbf{E}, \, x' \gg d, \quad (42)$$

where $v_n = \mathrm{i}\omega u_n$ is the normal velocity, d is a characteristic dimension of the structure, and α is the angle between the vectors $\mathbf{x}$ and $\mathbf{x}'$ (Fig. 2).

FLUID–STRUCTURE EIGENVALUE PROBLEMS AND ADDED MASS

Another problem of interest in numerical structural acoustics is that of computing the natural vibrational frequencies of general submerged structures. At low frequencies, the fluid appears to the structure like an added mass [47]; i.e. the fluid pressure on the wet surface is in phase with structural acceleration. At higher frequencies, the fluid impedance (the ratio of fluid pressure to velocity) is mathematically complex, since it involves both mass-like and damping-like effects. The primary difference between these two situations from a computational point of view is that the low frequency calculation can be performed using standard real eigenvalue analysis. In addition, as frequency increases, the added mass effects diminish and the damping (or piston) effects increase, so that the interpretation of the complex eigenvectors as "normal modes" becomes more difficult. For shell structures, these complications become somewhat academic, since shells have high modal density above

the first few modes, making the usefulness of computing such modes in doubt.

In this section, we consider the general fluid–structure eigenvalue problem for both compressible and incompressible fluids. In both cases, a structure's fluid-loaded modes are different from the *in-vacuo* modes, so that fully-coupled calculations are required. For an incompressible fluid (with sound speed $c \to \infty$), the fluid pressure satisfies Laplace's equation, and the effect of the fluid on the structure is that of added mass, the effects of which can be computed using either finite element or boundary element techniques, among others.

Finite element approaches

Both the pressure formulation, eqn (21), and the velocity potential formulation, eqn (25), can be the basis for a complex eigenvalue problem. With zero right-hand sides and $p_s = p$, the eigenvalue problems for a damped structure coupled to a compressible fluid are therefore

$$\begin{bmatrix} M & 0 \\ -\rho L^T & Q \end{bmatrix} \begin{Bmatrix} \ddot{u} \\ \ddot{p} \end{Bmatrix} + \begin{bmatrix} B & 0 \\ 0 & C \end{bmatrix} \begin{Bmatrix} \dot{u} \\ \dot{p} \end{Bmatrix}$$

$$+ \begin{bmatrix} K & L \\ 0 & H \end{bmatrix} \begin{Bmatrix} u \\ p \end{Bmatrix} = \begin{Bmatrix} 0 \\ 0 \end{Bmatrix} \quad (43)$$

for the pressure formulation, and

$$\begin{bmatrix} M & 0 \\ 0 & Q \end{bmatrix} \begin{Bmatrix} \ddot{u} \\ \ddot{q} \end{Bmatrix} + \begin{bmatrix} B & L \\ L^T & C \end{bmatrix} \begin{Bmatrix} \dot{u} \\ \dot{q} \end{Bmatrix}$$

$$+ \begin{bmatrix} K & 0 \\ 0 & H \end{bmatrix} \begin{Bmatrix} u \\ q \end{Bmatrix} = \begin{Bmatrix} 0 \\ 0 \end{Bmatrix}, \quad (44)$$

for the velocity potential formulation, where $u = u_0 e^{(\alpha + i\omega)t}$, K can be complex, B arises from viscous dampers, and C arises from the approximate radiation boundary condition at an artificial boundary. Both these forms can be solved using the complex eigenvalue routines in many standard finite element computer programs. Of the two approaches, the velocity potential approach, eqn (44), is generally preferred because of the symmetric coefficient matrices.

For undamped systems ($B = C = 0$, and K real), these two eigenvalue problems yield real natural frequencies, in spite of the nonsymmetry of eqn (43) and the presence of a "damping" matrix in eqn (44). Even in the undamped case, these two eigenvalue formulations are not attractive from a computational point of view, since, for most general finite element programs, both would require a complex eigensolver [to handle the nonsymmetry of eqn (43) and the "damping" matrix in eqn (44)]. Another variation of the undamped eigensystem results if the fluid

modulus in the velocity potential formulation is chosen as $G_e = 1/\rho$ rather than as in eqn (24)

$$\begin{bmatrix} M & 0 \\ 0 & Q \end{bmatrix} \begin{Bmatrix} \ddot{u} \\ \ddot{q} \end{Bmatrix} + \begin{bmatrix} 0 & L \\ -L^T & 0 \end{bmatrix} \begin{Bmatrix} \dot{u} \\ \dot{q} \end{Bmatrix}$$

$$+ \begin{bmatrix} K & 0 \\ 0 & H \end{bmatrix} \begin{Bmatrix} u \\ q \end{Bmatrix} = \begin{Bmatrix} 0 \\ 0 \end{Bmatrix}, \quad (45)$$

This skew-symmetry of the fluid–structure coupling is characteristic of gyroscopic systems [48], for which special eigensolution techniques have been developed [49].

The undamped fluid–structure eigenvalue problem can be symmetrized in standard form (i.e. with no "damping" matrix) by using the three-field formulation suggested by Morand and Ohayon [50], who combined the structural displacement u, fluid pressure p, and fluid displacement potential Ψ (whose gradient is displacement). From eqn (26), the relationship between pressure and displacement potential is

$$p = -\rho \ddot{\psi}, \quad (46)$$

which can be substituted into the two partitions of eqn (43) (with $B = C = 0$) to obtain

$$M\ddot{u} + Ku - \rho L\ddot{\psi} = 0 \quad (47)$$

and

$$\rho L\psi + Qp - \rho Hp = 0 \quad (48)$$

These two equations can be combined with eqn (46) (multiplied by Q) to yield [50]

$$\begin{bmatrix} M & 0 & -\rho L \\ 0 & 0 & Q \\ -\rho L^T & Q & -\rho H \end{bmatrix} \begin{Bmatrix} \ddot{u} \\ \ddot{p} \\ \ddot{\psi} \end{Bmatrix}$$

$$+ \begin{bmatrix} K & 0 & 0 \\ 0 & Q/\rho & 0 \\ 0 & 0 & 0 \end{bmatrix} \begin{Bmatrix} u \\ p \\ \psi \end{Bmatrix} = \begin{Bmatrix} 0 \\ 0 \\ 0 \end{Bmatrix}. \quad (49)$$

The above eigenvalue formulations are all for compressible fluids. For an incompressible fluid (for which the sound speed c is infinite), the fluid matrix Q vanishes, there are no waves in the fluid, and hence there is no need for a radiation boundary condition (i.e. $C = 0$). (In fact, it suffices to use the pressure release condition, $p = 0$, on the outer boundary of an exterior incompressible fluid.) In that case, the pressure formulation, eqn (43) simplifies to

$$\begin{bmatrix} M & 0 \\ -\rho L^T & 0 \end{bmatrix} \begin{Bmatrix} \ddot{u} \\ \ddot{p} \end{Bmatrix} + \begin{bmatrix} K & L \\ 0 & H \end{bmatrix} \begin{Bmatrix} u \\ p \end{Bmatrix} = \begin{Bmatrix} 0 \\ 0 \end{Bmatrix}, \quad (50)$$

from which we can eliminate pressure **p** to yield

$$(\mathbf{M} + \mathbf{M}_a)\ddot{\mathbf{u}} + \mathbf{K}\mathbf{u} = 0, \qquad (51)$$

where the symmetric, nonbanded matrix

$$\mathbf{M}_a = \rho \mathbf{L} \mathbf{H}^{-1} \mathbf{L}^{\mathsf{T}} \qquad (52)$$

is referred to as the added mass matrix. Using eqn (22), we could alternatively write the added mass matrix in terms of the normal d.f. at the wet points

$$\mathbf{M}_n = \rho \mathbf{A} \mathbf{H}^{-1} \mathbf{A}, \qquad (53)$$

where

$$\mathbf{M}_a = \mathbf{G} \mathbf{M}_n \mathbf{G}^{\mathsf{T}}. \qquad (54)$$

$\mathbf{M}_a$ has dimension equal to the number of structural d.f. in the entire model, and $\mathbf{M}_n$ has dimension equal to the number of points on the fluid–structure interface.

The low frequency (added mass) vibration problem can thus be solved by use of the pressure formulation [eqn (5)], the symmetric potential formulation [eqn (44) with $\mathbf{Q} = \mathbf{B} = \mathbf{C} = 0$], the three-field formulation [eqn (49) with $\mathbf{Q} = 0$], or the added mass formulation [eqn (51). Although all these forms are theoretically equivalent, the last two have the advantage of being in standard form for a real eigenvalue problem. Moreover, the added mass approach, eqn (51), allows the added mass matrix to be calculated using any suitable approach, including boundary elements or finite elements. However, eqn (51) has a considerable disadvantage in that matrix bandedness is destroyed, since $\mathbf{M}_a$ couples all wet d.f. to each other. Equations (44) and (50), on the other hand, have many more d.f. than eqn (51), but have banded coefficient matrices (if the structure and fluid unknowns are properly sequenced).

Boundary element approaches

The added mass matrix in eqn (51) can also be obtained by boundary element techniques. Since a solution to Laplace's equation is required, the technique of DeRuntz and Geers [51] would be applicable. Alternatively, the added mass matrix could be computed using a boundary element capability for the Helmholtz equation in the low frequency limit [52].

From the boundary element equation, eqn (40), with the incident pressure $\mathbf{p}_I = 0$, we have

$$\mathbf{p} = \mathbf{E}^{-1} \mathbf{C} \ddot{\mathbf{u}}_n, \qquad (55)$$

where $\ddot{\mathbf{u}}_n$ is the normal acceleration vector. Hence, the added mass matrix, which converts fluid acceleration to force, is, in terms of the fluid d.f.

$$\mathbf{M}_n = \mathbf{A} \mathbf{E}^{-1} \mathbf{C}, \qquad (56)$$

where **A** is the area matrix (of dimension $f \times f$) for the wet surface. As defined in this equation, $\mathbf{M}_n$ is full, symmetric, frequency-dependent and complex. The low frequency (incompressible fluid) added mass matrix is obtained by evaluating $\mathbf{M}_n$ in the limit $\omega \to 0$. Inspection of the Helmholtz integral equation eqn (30), indicates that, for small frequency, both **E** and **C** are real and constant. Thus, to compute $\mathbf{M}_n$ in eqn (56), only the real parts of **E** and **C** for small ω are considered. With this interpretation, the added mass matrix $\mathbf{M}_n$ is now full, symmetric, real and independent of frequency. In terms of the f structural d.f., we use the transformation matrix **G**, defined in eqns (14) and (19) to obtain

$$\mathbf{M}_a = \mathbf{G} \mathbf{A} \mathbf{E}^{-1} \mathbf{C} \mathbf{G}^{\mathsf{T}}, \qquad (57)$$

where $\mathbf{G}\mathbf{A} = \mathbf{L}$ from eqn (22). Here again, only the real parts of **E** and **C** for small ω are considered. The matrices $\mathbf{M}_n$ and $\mathbf{M}_a$ defined in eqns (56) and (57) are the boundary element equivalents of the finite element matrices of the same names defined in eqns (53) and (52). $\mathbf{M}_n$ and $\mathbf{M}_a$ are real, symmetric, nonbanded and independent of frequency. [The symmetry, while not obvious from eqns (56) and (57), follows from reciprocity considerations.]

The above boundary element procedure is applicable only for incompressible fluids, since, otherwise, fluid matrices **E** and **C** in eqn (57) would be frequency-dependent, and the eigenvalue problem eqn (51), would be nonlinear and not suitable for standard finite element packages. The finite element formulations, however, are applicable for either incompressible or compressible fluids.

INTERIOR FLUID PROBLEMS AND PIPING SYSTEMS

The foregoing finite element formulations, developed for the more complicated case of exterior fluids, are also applicable to fluid–structure problems with interior fluids. The two main simplifications associated with interior fluids are that there is no need to introduce an artificial boundary with a nonreflecting boundary condition, and, for scattering problems, there is no decomposition of fluid pressure into incident and scattered components. In addition, the boundary element formulation presented above for exterior fluids is also applicable to interior fluids if the incident pressure $\mathbf{p}_I$ in eqn (35) is set to zero, and the normal **n** in Fig. 2 is always directed from the structure into the fluid [26].

The rest of this section will be devoted to the prediction of the dynamic response of fluid-filled piping systems, since these problems can often be solved without resorting to complex three-dimensional finite element analyis. The interesting

dynamic behavior includes both water hammer (a transient phenomenon) and the steady-state (time-harmonic) vibrations caused by unbalanced rotating machinery such as pumps, for example.

Although the finite element procedures presented in this paper are applicable to piping systems, simplified beam models suffice for the relatively low frequencies which are often of interest [53, 54]. Low frequency dynamic behavior is characterized by pipes which respond only in their beam (rather than lobar) modes and by fluid wavelengths which are large compared to the pipe diameter. Thus, for such situations, the fluid wave propagation is essentially planar.

Finite element beam modeling of low frequency dynamic response of fluid-filled elastic piping systems typically takes the following approach [55, 56]. For structural acoustic response, it is assumed that the average flow speed is so small compared to the sound speed that the acoustic response is unaffected. Except for inertial effects, the fluid–structure coupling is assumed to occur only at pipe bends and other joints. Thus, fluid is allowed to slide without friction in straight sections of pipe. The equation satisfied by either the fluid pressure or the axial component of fluid displacement is the scalar wave equation, eqn (1). Thus the fluid can be modeled by an axial structural member (a rod element).

Beam finite elements are used to model both the straight sections and the elbows. Since a pipe bend is more flexible than an equivalent length of straight pipe, the moments of inertia for the beam elements in each elbow are divided by the appropriate flexibility factor (a standard correction applied to beam models of curved pipe).

For the acoustic fluid inside the pipe, a duplicate set of grid points is defined to coincide with the pipe grid points. The fluid is modeled with elastic rod elements, which are equivalent to beam elements with zero flexural and torsional stiffness. These elements are assigned the actual mass density ρ for the fluid and a Young's modulus E given by

$$E = B/[1 + BD/(E_s t)], \qquad (58)$$

where B is the fluid bulk modulus of elasticity, D is the mean diameter of the pipe, E_s is the Young's modulus of the pipe material, and t is the pipe wall thickness. The denominator in this equation is a corrective factor which accounts for the elasticity of the pipe [57, 58]. The practical effect of the corrective factor is to reduce the apparent speed of propagation of longitudinal waves in the fluid because of the elasticity of the pipe walls.

The fluid, which is modeled with axial members, has only one independent d.f. at each grid point. The three rotational d.f. are restrained at all fluid points. Both transverse translational d.f. at each fluid point are constrained to move with the corresponding

structural point. The only remaining d.f., the axial displacement, is free to slide relative to the pipe. These constraints are applicable in both the straight sections and the elbows. The fluid pressure can be recovered from the finite element program as the stress.

This approach to low frequency modeling of piping [56] can be applied using many general purpose finite element structural analysis codes. The resulting model has seven independent d.f. at each grid point location, six for the pipe and one for the axial component of fluid displacement. To reduce matrix bandwidth or profile, each fluid grid point can be sequenced adjacent to its corresponding structural point.

For the finite element dynamic response prediction of piping systems at higher frequencies for which beam models are not valid, general three-dimensional models are required. In general, this approach models the pipe with shell elements and the contained fluid with three-dimensional finite elements, as described earlier in this paper.

DOUBLY ASYMPTOTIC FLUID APPROXIMATIONS

The mathematically exact integral representation for an exterior infinite fluid in transient fluid–structure interaction problems is the retarded potential integral equation. The total pressure p on the wet surface S of an elastic structure subjected to an incident pressure is given by [59–62]

$$p(\mathbf{r}, t) = 2p_i(\mathbf{r}, t) - \frac{\rho}{2\pi} \int_S \frac{\ddot{w}(\mathbf{r}', t')}{R} \, dS'$$

$$+ \frac{1}{2\pi} \int_S \left[p(\mathbf{r}', t') + \frac{R}{c} \frac{\partial p(\mathbf{r}', t')}{\partial t'} \right] \frac{1}{R^2} \frac{\partial R}{\partial n'} \, dS', \quad (59)$$

where p_i is the incident pressure in the fluid, ρ is the fluid density, c is the speed of sound in the fluid, $\mathbf{r}$ is a field point on the surface, $\mathbf{r}'$ is an integration point on the surface, $R = |\mathbf{r} - \mathbf{r}'|$, $t' = t - R/c$ is the retarded time of the integration point, $\mathbf{n}'$ is the outward normal (from the fluid) at an integration point, and $\ddot{w}$ is the normal component of acceleration. In applications, this integral equation is discretized and solved simultaneously with the finite element equations for the structure.

Since this calculation of surface pressure is nonlocal in both space and time, it is seldom used in practice. An attractive alternative, at least for shock problems (where the principle interest is in structural response), is provided by fluid loading approximations such as the doubly asymptotic approximations [47, 63–65]. The lower order approximation, referred to as DAA1, is a matrix differential equation

relating surface scattered pressure and structural motion:

$$\dot{\mathbf{p}}_s + \rho c \mathbf{M}_n^{-1} \mathbf{A} \mathbf{p}_s = \rho c \ddot{\mathbf{u}}_{ns}, \tag{60}$$

where $\mathbf{p}_s$ is the scattered pressure [eqn (13)] on the wet surface of the structure, $\mathbf{M}_n$ is the (full) added mass matrix for the wet surface of the structure, $\mathbf{A}$ is the area matrix converting grid point pressures to normal forces on the wet surface, and $\ddot{\mathbf{u}}_{ns}$ is the normal component of scattered wave particle accelerations on the wet surface. This system has dimension equal to the number of wet grid points on the fluid–structure interface.

Equation (60) was designated "doubly asymptotic" because it exhibits the correct asymptotic behavior at both the low and high frequency limits and provides a smooth transition in the intermediate frequency range. For low frequencies (late time), the second term of eqn (60) dominates the first term, yielding the virtual mass approximation. At high frequencies (early time), the first term dominates the second, yielding the plane wave approximation ($p = \rho c v$).

Surface motions, like pressures in eqn (13), can be decomposed into incident and scattered components. Thus,

$$\ddot{\mathbf{u}}_{ns} = \ddot{\mathbf{u}}_n - \ddot{\mathbf{u}}_{ni} = \mathbf{G}^T \ddot{\mathbf{u}} - \ddot{\mathbf{u}}_{ni}, \tag{61}$$

where the second part of this equation follows from eqn (19). If a change of variable is made to scattered velocity potential q [eqn (23), eqn (60) becomes

$$\dot{\mathbf{q}} + \rho c \mathbf{M}_n^{-1} \mathbf{A} \mathbf{q} = \rho c (\mathbf{G}^T \dot{\mathbf{u}} - \mathbf{v}_{ni}), \tag{62}$$

where $\mathbf{v}_{ni} = \dot{\mathbf{u}}_{ni}$. If this equation is then multiplied by $-\mathbf{A}/\rho c$ and combined with eqns (14) (for the structure) and (22), one obtains, for the coupled fluid–structure system [66, 67]

$$\begin{bmatrix} \mathbf{M} & \mathbf{0} \\ \mathbf{0} & \mathbf{0} \end{bmatrix} \begin{Bmatrix} \ddot{\mathbf{u}} \\ \ddot{\mathbf{q}} \end{Bmatrix} + \begin{bmatrix} \mathbf{B} & \mathbf{L} \\ \mathbf{L}^T & -\mathbf{A}/\rho c \end{bmatrix} \begin{Bmatrix} \dot{\mathbf{u}} \\ \dot{\mathbf{q}} \end{Bmatrix}$$

$$+ \begin{bmatrix} \mathbf{K} & \mathbf{0} \\ \mathbf{0} & -\mathbf{A}\mathbf{M}_n^{-1}\mathbf{A} \end{bmatrix} \begin{Bmatrix} \mathbf{u} \\ \mathbf{q} \end{Bmatrix} = \begin{Bmatrix} \mathbf{F} - \mathbf{L}\mathbf{p}_i \\ \mathbf{A}\mathbf{v}_{ni} \end{Bmatrix}, \tag{63}$$

where $\mathbf{A}$ has nonzeros only on the wet surface (the fluid–structure interface). This equation shows one approach for coupling DAA1 to finite element structural equations.

As was pointed out in the discussion of the symmetric velocity potential formulation, the use of velocity potential as the fundamental fluid unknown results in an excitation on the right-hand side of eqn (63) which is proportional to incident fluid particle velocity rather than acceleration. Velocity is preferable to acceleration for shock problems, since such problems often have incident pressure loadings with

a simple jump discontinuity, which makes the acceleration discontinuity a Dirac delta.

The added mass matrix $\mathbf{M}_n$ in the DAA1 formulation, eqn (63), can be computed by either boundary element [eqn (56)] or finite element [eqn (53)] techniques, among others. If boundary elements are used [51, 52], the matrix product $\mathbf{A}\mathbf{M}_n^{-1}\mathbf{A}$ must be computed, where $\mathbf{M}_n$ is fully populated and equal in dimension to the number of fluid d.f. on the fluid–structure interface. On the other hand, if a finite element model of a portion of exterior fluid is used to compute the added mass matrix, the coupled system, eqn (63) simplifies to

$$\begin{bmatrix} \mathbf{M} & \mathbf{0} \\ \mathbf{0} & \mathbf{0} \end{bmatrix} \begin{Bmatrix} \ddot{\mathbf{u}} \\ \ddot{\mathbf{q}} \end{Bmatrix} + \begin{bmatrix} \mathbf{B} & \mathbf{L} \\ \mathbf{L}^T & -\mathbf{A}/\rho c \end{bmatrix} \begin{Bmatrix} \dot{\mathbf{u}} \\ \dot{\mathbf{q}} \end{Bmatrix}$$

$$+ \begin{bmatrix} \mathbf{K} & \mathbf{0} \\ \mathbf{0} & -\mathbf{H}/\rho \end{bmatrix} \begin{Bmatrix} \mathbf{u} \\ \mathbf{q} \end{Bmatrix} = \begin{Bmatrix} \mathbf{F} - \mathbf{L}\mathbf{p}_i \\ \mathbf{A}\mathbf{v}_{ni} \end{Bmatrix}, \tag{64}$$

where eqn (53) was used. In this case, the added mass effects require only the assembly of a finite element "stiffness" matrix ($\mathbf{H}$) for the fluid domain, and no inversion of a full added mass matrix is needed.

As given in eqn (64), the fluid "stiffness" matrix $\mathbf{H}$ is, in effect, the result of a static condensation of the larger, banded matrix computed for the entire fluid domain. Since the nonzeros in the fluid partition of eqn (64) are associated only with interface d. f., $\mathbf{H}$ could be left in expanded form and not condensed to the wet surface. In this case, $\mathbf{q}$'s dimension would increase to the total number of fluid d.f. in the exterior fluid domain, but $\mathbf{H}$ would be sparse, and the equation could then be readily solved using standard finite element packages (if the structure and fluid unknowns were interspersed in their numbering, if necessary, to minimize matrix bandwidth or profile).

We note also the similarity between the DAA1 formulation, eqn (64), and the finite element velocity potential formulation, eqn (25). The DAA1 formulation has no fluid "inertia" matrix $\mathbf{Q}$, since an incompressible fluid domain is modelled to obtain added mass effects. The damping matrices differ only in the lower right partition, since the DAA1 dampers are placed on the fluid d.f. at the fluid–structure interface, and the compressible fluid velocity potential formulation places a radiation boundary condition on the outer fluid boundary. If the first-order plane wave approximation is used in eqn (25), the same fluid "dashpots" ($-\mathbf{A}/\rho c$) are used in both cases. The stiffness matrices in eqns (25) and (64) are identical, since, in eqn (25), the multiplicative constant $-1/\rho$ has already been absorbed into the matrix $\mathbf{H}$. However, the mesh requirements for $\mathbf{H}$ in eqns (25) and (64) are not the same, since the compressible fluid of eqn (25) would require a mesh density and extent suitable for the propagation of

acoustic waves of various lengths. The mesh used for eqn (64) needs only to be adequate to solve Laplace's equation in the exterior domain.

If the DAA1 equations are solved with boundary element calculation of the added mass matrix, it is often convenient [68] to uncouple the fluid and structure partitions on the left-hand side of eqn (63) by moving the coupling terms (matrix **L**) to the right-hand side as solution-dependent pseudo-loads. In this case, numerical stability suffers, and the stabilization procedures of Park *et al.* [69] could be used.

FLUID INFINITE ELEMENT MODELING

The principle computational tradeoff between a fluid finite element approach for exterior problems and the boundary element approach is that the finite element approach yields large, banded matrices, whereas the boundary element approach yields smaller, densely-populated matrices. This trade-off often favors the finite element approach for long, slender structures likes ships which are "naturally banded". In addition, only the fluid finite element approach has directly available an explict fluid mesh which can be used for graphical display of the wave motion through the fluid. The principal drawbacks to a fluid finite element approach are the need for an approximate radiation boundary condition at the outer fluid boundary, the requirements on mesh size and extent (sometimes leading to frequency-dependent fluid meshes [9]), and the difficulty of generating the fluid mesh.

A compromise between the accuracy of the boundary element fluid model and the computational efficiency of the finite element model is perhaps provided by fluid infinite elements. The strengths of fluid infinite elements are that they provide a better radiation boundary condition on the outer boundary of a fluid finite element mesh than is provided by the plane wave approximation, and they preserve the symmetric, banded character of conventional finite element formulations. The typical way in which infinite elements are used in structural acoustics is that the structure and a small portion of exterior fluid are modeled with finite elements, outside of which a layer of infinite fluid elements is added. The outer boundary of the fluid finite elements (i.e. the inner boundary of the layer of infinite elements) is required to be convex.

Although a variety of infinite element shape functions has been proposed [27–31], the concern here is only with the coupling of the infinite element matrices into fluid-structure interaction analysis. It is convenient to view the infinite element formulation as a variation of the finite element symmetric potential formulation, eqn (25), except that matrix **C**, which arises in eqn (25) from the approximate radiation boundary condition on the outer fluid boundary, is deleted, and the fluid "stiffness" matrix **H** has

contributions from fluid finite elements and the infinite elements which are placed outside the fluid finite elements

$$
\begin{bmatrix} \mathbf{M} & \mathbf{0} \\ \mathbf{0} & \mathbf{Q} \end{bmatrix} \begin{Bmatrix} \ddot{\mathbf{u}} \\ \ddot{\mathbf{q}} \end{Bmatrix} + \begin{bmatrix} \mathbf{B} & \mathbf{L} \\ \mathbf{L}^T & \mathbf{0} \end{bmatrix} \begin{Bmatrix} \dot{\mathbf{u}} \\ \dot{\mathbf{q}} \end{Bmatrix}
$$

$$
+ \begin{bmatrix} \mathbf{K} & \mathbf{0} \\ \mathbf{0} & \mathbf{H}_{FE} + \mathbf{H}_{IE} \end{bmatrix} \begin{Bmatrix} \mathbf{u} \\ \mathbf{q} \end{Bmatrix} = \begin{Bmatrix} \mathbf{F} - \mathbf{L}\mathbf{p}_i \\ \mathbf{A}v_{ni} \end{Bmatrix}, \quad (65)
$$

where $\mathbf{H}_{FE}$ is the frequency-independent fluid "stiffness" matrix assembed from the fluid finite elements, and $\mathbf{H}_{IE}$ is the symmetric, frequency-dependent matrix arising from the infinite elements. The set **q** of fluid unknowns is augmented, if necessary, to include infinite element mid-side nodes located "halfway" to infinity. In this symmetric formulation, $\mathbf{H}_{IE}$, like $\mathbf{H}_{FE}$, has the scalar multiplier $-1/\rho$ already absorbed. [That is, $\mathbf{H}_{IE}$ is obtained from an infinite element discretization of the Helmholtz equation, eqn (5), multiplied by $-1/\rho$.] Note that, although eqn (65) is written in the time domain, it has meaning only in the frequency domain, since $\mathbf{H}_{IE}$ is complex and frequency-dependent.

Equation (65) is solved using conventional direct frequency response approaches, except that the frequency-dependent infinite element matrix $\mathbf{H}_{IE}$ must be reassembled for each new drive frequency. With proper grid point sequencing, eqn (65) has the same banded structure as other finite element matrices.

DISCUSSION

Practical formulations have been summarized for finite element, boundary element, and infinite element modeling of fluid domains in contact with finite element structural models. Depending on the type of problem (transient, forced time-harmonic, or eigenvalue) and fluid (interior or exterior), there are several options for solving a given problem. Fluid finite element models can be used for all problems, although, for exterior fluids, an approximate radiation boundary condition is required. Fluid boundary elements can also be used for all problems, although the strength of boundary elements lies in the exterior problems. Until recently [70], infinite elements have been formulated for frequency domain analysis only. In addition, both boundary elements and infinite elements generate frequency-dependent matrices, so that eigenvalue problems based on these formulations would be nonlinear.

Transient and forced time-harmonic problems with an interior fluid can be conveniently solved using the symmetric finite element velocity potential formulation, in which each fluid mesh point is represented by a single d.f., and the resulting matrix system is both symmetric and banded (or sparse). However, for undamped time-harmonic problems, for which only

real equation solving is needed, the pressure formulation would be more economical than the symmetric velocity potential formulation if the finite element program has efficient nonsymmetric matrix routines.

Transient problems with an exterior fluid can be most accurately solved using the retarded potential integral equation for the fluid, but the relatively high computational cost associated with that approach often leads practitioners to use either fluid finite elements (with a simple radiation boundary condition) or, for linear shock problems, one of the doubly asymptotic approximations. The latter are rarely used for steady-state acoustic analysis.

Time-harmonic problems with an exterior fluid are also most accurately solved using a boundary element fluid model, but it is possible to get high accuracy at less computational cost if an infinite element fluid model is used instead, since this approach yields the symmetric, banded systems common to finite element analysis. The lowest computational costs and accuracies result from exterior fluid finite element models which are truncated with a simple nonreflecting boundary condition such as the plane wave absorbing boundary.

Damped eigenvalue problems, which are mathematically complex, can be conveniently solved using the symmetric velocity potential formulation, which assigns one d.f. to each fluid point and generates symmetric, banded matrices.

The most difficult choices arise with undamped eigenvalue problems, since there is no coupled fluid–structure formulation which uses a single scalar d.f. for each fluid point and which yields a real eigenproblem with symmetric, banded (or sparse) matrices. The three-field formulation of Morand and Ohayon is perhaps a good compromise, since it achieves a real, symmetric eigenproblem, but at the expense of an additional fluid d.f. at each fluid point and a wider matrix bandwidth.

REFERENCES

1. O. C. Zienkiewicz and R. E. Newton, Coupled vibrations of a structure submerged in a compressible fluid. In: *Proc. Int. Symp. on Finite Element Techniques* (Edited by M. Sorensen), pp. 359–379. University of Stuttgart, Stuttgart (1969).
2. A. Craggs, The transient response of a coupled plate-acoustic system using plate and acoustic finite elements. *J. Sound Vib.* **15** 509–528 (1971).
3. A. J. Kalinowski, Fluid structure interaction. In: *Shock and Vibration Computer Programs: Reviews and Summaries* (Edited by W. Pilkey and B. Pilkey), Vol. SVM-10, pp. 405–452. The Shock and Vibration Information Center, Naval Research Laboratory, Washington, DC (1975).
4. L. Kiefling and G. C. Feng, Fluid–structure finite element vibrational analysis. *AIAA J.* **14**, 199–203 (1976).
5. A. J. Kalinowski, Transmission of shock waves into submerged fluid filled vessels. In: *Fluid Structure Interaction Phenomena in Pressure Vessel and Piping Systems* (Edited by M. K. Au-Yang and S. J. Brown,

Jr), pp. 83–105. The American Society of Mechanical Engineers, New York (1977).
6. O. C. Zienkiewicz and P. Bettess, Fluid–structure dynamic interaction and wave forces: an introduction to numerical treatment. *Int. J. numer. Meth. Engng.* **13**, 1–6 (1978).
7. M. A. Hamdi and Y. Ousset, A displacement method for the analysis of vibrations of coupled fluid–structure systems. *Int. J. numer. Meth. Engng.* **13**, 139–150 (1978).
8. R. E. Newton, *Finite Element Study of Shock Induced Cavitation*. American Society of Civil Engineers, New York (1980).
9. A. J. Kalinowski and C. W. Nebelung, Media-structure interaction computations employing frequency-dependent mesh size with the finite element method. *Shock Vibr. Bull* **51**, 173–193 (1981).
10. G. C. Everstine, A symmetric potential formulation for fluid–structure interaction. *J. Sound Vib.* **79**, 157–160 (1981).
11. G. C. Everstine, Structural-acoustic finite element analysis, with application to scattering. In: *Proc. 6th Invitational Symp. on the Unification of Finite Elements, Finite Differences, and Calculus of Variations* (Edited by H. Kardestuncer) pp. 101–122. University of Connecticut, Storrs, CT (1982).
12. P. M. Pinsky and N. N. Abboud, Transient finite element analysis of the exterior structural acoustics problem. In: *Numerical Techniques in Acoustic Radiation* (Edited by R. J. Bernhard and R. F. Keltie), NCA-Vol. 6, pp. 35–47. American Society of Mechanical Engineers, New York (1989).
13. H. C. Chen and R. L. Taylor, Vibration analysis of fluid–solid systems using a finite element displacement formulation. *Int. J. numer. Meth. Engng.* **29**, 683–698 (1990).
14. L. H. Chen and D. G. Schweikert, Sound radiation from an arbitrary body. *J. Acoust. Soc. Am.* **35**, 1626–1632 (1963).
15. H. A. Schenck, Improved integral formulation for acoustic radiation problems. *J. Acoust. Soc. Am.* **44**, 41–58 (1968).
16. G. Chertock, Integral equation methods in sound radiation and scattering from arbitrary surfaces. Report 3538, Naval Ship Research and Development Center, Bethesda, MD (1971).
17. A. J. Burton and G. F. Miller, The application of integral equation methods to the numerical solution of some exterior boundary-value problems. *Proc. R. Soc. Lond. A* **323**, 201–210 (1971).
18. J. J. Engblom and R. B. Nelson, Consistent formulation of sound radiation from arbitrary structure. *J. appl. Mech.* **42**, 295–300 (1975).
19. D. T. Wilton, Acoustic radiation and scattering from elastic structures. *Int. J. numer. Meth. Engng.* **13**, 123–138 (1978).
20. J. S. Patel, Radiation and scattering from an arbitrary elastic structure using consistent fluid structure formulation. *Comput. Struct.* **9**, 287–291 (1978).
21. I. C. Mathews, Numerical techniques for three-dimensional steady-state fluid–structure interaction. *J. Acoust. Soc. Am.* **79**, 1317–1325 (1986).
22. M. Rezayat, D. J. Shippy and F. J. Rizzo, On time-harmonic elastic-wave analysis by the boundary element method for moderate to high frequencies. *Comput. Meth. appl. Mech. Engng.* **55**, 349–367 (1986).
23. A. F. Seybert, B. Soenarko, F. J. Rizzo and D. J. Shippy, A special integral equation formulation for acoustic radiation and scattering for axisymmetric bodies and boundary conditions. *J. Acoust. Soc. Am.* **80**, 1241–1247 (1986).
24. A. F. Seybert, T. W. Wu and X. F. Wu, Radiation and scattering of acoustic waves from elastic solids and

shells using the boundary element method. *J. Acoust. Soc. Am.* **84**, 1906–1912 (1988).

25. G. C. Everstine and F. M. Henderson, Coupled finite element/boundary element approach for fluid–structure interaction. *J. Acoust. Soc. Am.* **87**, 1938–1947 (1990).

26. G. C. Everstine and R. S. Cheng, The coupling of finite elements and boundary elements for scattering from fluid-filled structures. In: *Computer Technology: Advances and Applications*, PVP-Vol. 234, pp. 43–47. American Society of Mechanical Engineers, New York (1992).

27. P. Bettess, Infinite elements. *Int. J. numer. Meth. Engng.* **11**, 53–64 (1977).

28. P. Bettess, More on infinite elements. *Int. J. numer. Meth. Engng.* **15**, 1613–1626 (1977).

29. O. C. Zienkiewicz, C. Emson and P. Bettess, A novel boundary infinite element. *Int. J. numer. Meth. Engng.* **19**, 393–404 (1983).

30. O. C. Zienkiewicz, K. Bando, P. Bettess and T. C. Chiam, Mapped infinite elements for exterior wave problems. *Int. J. numer. Meth. Engng.* **21**, 1229–1251 (1985).

31. E. T. Moyer, Jr, Performance of mapped infinite elements for exterior wave scattering applications. *Commun. appl. numer. Meth.* **8**, 27–39 (1992).

32. A. Bostrom, Scattering of stationary acoustic waves by an elastic obstacle immersed in water. *J. Acoust. Soc. Am.* **67**, 390–398 (1980).

33. M. F. Werby and L. H. Green, An extended unitary approach for acoustical scattering from elastic structures. *J. Acoust. Soc. Am.* **74**, 625–630 (1983).

34. M. F. Werby and G. J. Tango, Application of the extended boundary condition equations to scattering from fluid-loaded objects. *Engng. Anal.* **5**, 12–20 (1988).

35. J. T. Hunt, M. R. Knittel and D. Barach, Finite element approach to acoustic radiation from elastic structures. *J. Acoust. Soc. Am.* **55**, 269–280 (1974).

36. J. T. Hunt, M. R. Knittel, C. S. Nichols and D. Barach, Finite-element approach to acoustic scattering from elastic structures. *J. Acoust. Soc. Am.* **57**, 287–299 (1975).

37. J. B. Keller and D. Givoli, Exact non-reflecting boundary conditions. *J. Comput. Phys.* **82**, 172–192 (1989).

38. I. S. Sokolnikoff, *Theory of Elasticity*, 2nd Edn. McGraw-Hill, New York (1956).

39. L. E. Kinsler, A. R. Frey, A. B. Coppens and J. V. Sanders, *Fundamentals of Acoustics*, 3rd Edn. Wiley, New York (1982).

40. M. C. Junger and D. Feit, *Sound, Structures, and Their Interaction*, 2nd Edn. The MIT Press, Cambridge, MA (1986).

41. K. H. Huebner and E. A. Thornton, *The Finite Element Method for Engineers*, 2nd Edn. Wiley, New York (1982).

42. G. C. Everstine, Structural analogies for scalar field problems. *Int. J. numer. Meth. Engng.* **17**, 471–476 (1981).

43. J. Lysmer and R. L. Kuhlemeyer, Finite dynamic model for infinite media. *J. Engng. Mech. Div. ASCE* **95** (EM4), 859–877 (1969).

44. A. Bayliss and E. Turkel, Radiation boundary conditions for wave-like equations. *Commun. Pure Appl. Math.* **XXXIII** 707–725 (1980).

45. R. H. Cole, *Underwater Explosions*. Princeton University Press, Princeton, NJ (1948).

46. G. C. Everstine, Treatment of static preload effects in acoustic radiation and scattering. *Sixteenth NASTRAN Users' Colloquium*, NASA CP-2505, National Aeronautics and Space Administration, Washington, DC, pp. 138–152 (1988).

47. T. L. Geers, Residual potential and approximate methods for three-dimensional fluid–structure interaction problems. *J. Acoust. Soc. Am.* **49**, 1505–1510 (1971).

48. E. H. Dowell, G. F. Gorman, III and D. A. Smith, Acoustoelasticity: general theory, acoustic natural modes and forced responses to sinusoidal excitation, including comparisons with experiment. *J. Sound Vib.* **52**, 519–542 (1977).

49. L. Meirovitch, A new method of solution of the eigenvalue problem for gyroscopic systems. *AIAA J.* **12**, 1337–1342 (1974).

50. H. Morand and R. Ohayon, Substructure variational analysis of the vibrations of coupled fluid–structure systems. Finite element results. *Int. J. numer. Meth. Engng.* **14**, 741–755 (1979).

51. J. A. DeRuntz and T. L. Geers, Added mass computation by the boundary element method. *Int. J. numer. Meth. Engng.* **12**, 531–549 (1978).

52. G. C. Everstine, Prediction of low frequency vibrational frequencies of submerged structures. *J. Vibr. Acoustics* **113**, 187–191 (1991).

53. L. C. Davidson and J. E. Smith, Liquid–structure coupling in curved pipes. *Shock Vibr. Bull.* **40**, 197–207 (1969).

54. L. C. Davidson and D. R. Samsury, Liquid–structure coupling in curved pipes—II. *Shock Vibr. Bull.* **42**, 123–136 (1972).

55. R. E. Schwirian and M. E. Karabin, Use of spar elements to simulate fluid–solid interaction in the finite element analysis of piping system dynamics. *Nucl. Engng. Des.* **66**, 47–59 (1981).

56. G. C. Everstine, Dynamic analysis of fluid-filled piping systems using finite element techniques. *J. Press. Vessel Technol.* **108**, 57–61 (1986).

57. V. L. Streeter, *Fluid Mechanics*, 3rd Edn. McGraw-Hill, New York (1962).

58. N. Krause, W. Goldsmith and J. L. Sackman, Transients in tubes containing liquids. *Int. J. Mech. Sci.* **19**, 53–68 (1977).

59. H. Huang, G. C. Everstine and Y. F. Wang, Retarded potential techniques for the analysis of submerged structures impinged by weak shock waves. In: *Computational Methods for Fluid–Structure Interaction Problems* (Edited by T. Belytschko and T. L. Geers) AMD-Vol. 26, pp. 83–93. The American Society of Mechanical Engineers, New York (1977).

60. Y. P. Lu, The application of retarded potential techniques to submerged dynamic structural systems. In: *Innovative Numerical Analysis for the Engineering Sciences* (Edited by R. Shaw, W. Pilkey, B. Pilkey, R. Wilson, A. Lakis, A. Chaudouet and C. Marino) pp. 59–68. University Press of Virginia, Charlottesville, VA (1980).

61. M. A. Tamm and W. W. Webbon, Submerged structural response to weak shock by coupled three-dimensional retarded potential fluid analysis—finite element structural analysis. Memorandum Report 5903, Naval Research Laboratory, Washington, DC (1987).

62. M. A. Tamm, A parametric patch surface geometry definition for the three-dimensional retarded potential technique. Memorandum Report 5904, Naval Research Laboratory, Washington, DC (1987).

63. T. L. Geers, Doubly asymptotic approximations for transient motions of submerged structures. *J. Acoust. Soc. Am.* **64**, 1500–1508 (1978).

64. T. L. Geers and C. A. Felippa, Doubly asympotic approximations for vibration analysis of submerged structures. *J. Acoust. Soc. Am.* **73**, 1152–1159 (1983).

65. C. A. Felippa, Top-down derivation of doubly asymptotic approximations for structure–fluid interaction analysis. In: *Innovative Numerical Analysis for the*

Engineering Sciences (Edited by R. Shaw, W. Pilkey, B. Pilkey, R. Wilson, A. Lakis, A. Chaudouet and C. Marino), pp. 79–88. University Press of Virginia, Charlottesville, VA (1980).

66. G. C. Everstine, A NASTRAN implementation of the doubly asymptotic approximation for underwater shock response. In: *NASTRAN: Users' Experiences*, NASA TM X-3428, pp. 207–228. National Aeronautics and Space Administration, Washington, DC (1976).

67. H. C. Neilson, G. C. Everstine and Y. F. Wang, Transient response of a submerged fluid-coupled double-walled shell structure to a pressure pulse. *J. Acoust. Soc. Am.* **70**, 1776–1782 (1981).

68. J. A. DeRuntz, T. L. Geers and C. A. Felippa, The underwater shock analysis code (USA-Version 3): a reference manual. Report DNA-5615F, Lockheed Missiles and Space Co., Inc., Palo Alto, CA (1980).

69. K. C. Park, C. A. Felippa and J. A. DeRuntz, Stabilization of staggered solution procedures for fluid–structure interaction analysis. In: *Computational Methods for Fluid–Structure Interaction Problems* (Edited by T. Belytschko and T. L. Geers), AMD-Vol. 26, pp. 94–124. The American Society of Mechanical Engineers, New York (1977).

70. R. J. Astley, A transient infinite element for multi-dimensional acoustic radiation. In: *Acoustics of Submerged Structures and Transduction Systems* (Edited by R. P. Daddazio, M. M. Ettouney and N. N. Abboud). The American Society of Mechanical Engineers, New York (1995).